Chemical Engineering Journal 110 (2005) 101–111

Chemical Engineering Journal

www.elsevier.com/locate/cej

Adsorptive purification of phenol wastewaters: Experimental basis and operation of a parametric pumping unit

Marta Otero [1], Miriam Zabkova, Alírio E. Rodrigues *

Laboratory of Separation and Reaction Engineering (LSRE), Department of Chemical Engineering, Faculty of Engineering, University of Porto, 4200-465 Porto, Portugal

Received 3 September 2004; received in revised form 16 February 2005; accepted 18 February 2005

Abstract

Phenol is a target pollutant to be removed from wastewaters from different industries. Adsorption of phenol from aqueous solutions onto two polymeric resins (Sephabeads SP206 and SP207) and onto activated carbon (Filtrasorb F400) was studied. Batch equilibrium experiments were carried out at three different temperatures (293, 310 and 333 K) for each of the adsorbents. In order to ascertain the fixed bed performance of the adsorbents considered, adsorption runs were carried out at laboratory scale at 293, 310 and 333 K. Equilibrium and fixed bed experimental results were compared to the simulated ones. Equilibrium data were well fitted by the Langmuir isotherm and the breakthrough curves simulation was based on this equilibrium isotherm together with a mass transfer description based on the Linear Driving Force (LDF) model. After the adsorbents screening and mass transfer parameters determination, Sephabeads SP206 was used to purify a phenolic solution by parametric pumping at pilot scale using hot and cold temperatures of 293 and 333 K, respectively. A package for the simulation of this cyclic operation was used to predict model results, which were satisfactorily compared to those experimentally obtained.

Keywords: Phenol; Adsorption; Parametric pumping; Activated carbon; Polymeric adsorbents

1. Introduction

Among the environmentally concerned substances, phenols, which are considered highly toxic, are the most common pollutants [1,2]. Adsorptive processes are widely used in the purification of polluted streams and diluted wastewaters [3–5]. An interesting aspect of sorption operations is their ability to concentrate solutes. Conventional fixed bed processes involve a saturation, adsorption or loading step, followed by desorption, elution or regeneration steps. On the whole, wastewater purification by means of conventional fixed bed comprise two drawbacks, one is the low efficiency of the fixed bed operation, since only a fraction of the adsorbent is used and the other is the use of a chemical regenerant to get an operative bed, with the associate waste disposal and a new pollution problem.

Parametric pumping is a cyclic separation process in which a mobile phase percolates through a fixed bed upwards and downwards alternatively; a change in the temperature (or in another thermodynamic variables such as pressure, pH, etc.) occurring simultaneously with the change in the flow direction [6]. In thermal parametric pumping, the temperature is the changing variable and the process is based upon the fact that the adsorption equilibrium isotherm of solutes onto some materials changes with temperature. The temperature change may be either carried out by the solution itself (in “recuperative mode”), which is heated or cooled by means of thermostatic baths, or imposed through the column wall (in “direct mode”). Also data on the combination of both modes have been published [7] but, no matter the mode in which thermal parametric pumping is operated, thermal energy is used as regenerant. Under appropriate conditions, wastewater to be purified passes through a bed of adsorbent in upward flow at a temperature T_h (hot half-cycle) followed by downward flow at a temperature T_c ($T_c < T_h$) (cold half-cycle) which will produce a concentrated solution

* Corresponding author. Tel.: +351 225081671; fax: +351 225081674.
E-mail address: arodrig@fe.up.pt (A.E. Rodrigues).
[1] On leave of absence from Chemical Engineering Department, Natural Resources Institute, IRENA-ESTIA, University of León, Spain.

1385-8947/$ – see front matter © 2005 Elsevier B.V. All rights reserved.
doi:10.1016/j.cej.2005.02.033

Nomenclature

a	deviation in the separation parameter
A_w	wall specific area ($4/D$) (m^{-1})
ΔH_L	enthalpy of adsorption for the Langmuir isotherm ($J\,mol^{-1}$)
b	separation parameter
C	concentration in the bulk fluid phase ($g\,L^{-1}$)
C_0	initial liquid phase concentration of phenol in the batch and in the fixed bed operation ($mg\,L^{-1}$)
C_e	equilibrium liquid phase concentration of phenol ($mg\,L^{-1}$)
C_F	feed liquid phase concentration of phenol in the operation of the parametric pumping unit ($mg\,L^{-1}$)
Cp_f	heat capacity of the fluid (kJ/(kg K))
Cp_s	heat capacity of the solid (kJ/(kg K))
$\langle C_{BP}\rangle$	average concentration of the fluid in the bottom reservoir ($mg\,L^{-1}$)
$\langle C_{TP}\rangle$	average concentration of the fluid in the top reservoir ($mg\,L^{-1}$)
d_p	diameter of the particle of the adsorbent (cm)
D	bed diameter (mm)
D_{ax}	axial dispersion ($m^2\,min^{-1}$)
D_{pe}	the effective pore diffusivity ($m^2\,min^{-1}$)
D_m	the molecular diffusivity ($m^2\,min^{-1}$)
f_h	humidity factor ($g_{dry\ adsorbent}/g_{adsorbent}$)
h_w	wall heat transfer coefficient (kJ/(m^2 s K))
K_{ae}	axial thermal conductivity (kJ/(m s K))
K_L	parameter in the Langmuir isotherm model ($L\,mg^{-1}$)
K_L^∞	equilibrium constant corresponding to the Langmuir model ($L\,mg^{-1}$)
k_{LDF}	Linear Driving Force (LDF) kinetic rate constant (min^{-1})
L	bed length (m)
$\bar{m}(T)$	capacity parameter in the separation parameter b
m	average slope in the separation parameter b
M_B	molecular weight of solvent B ($g\,mol^{-1}$)
n	number of cycles
Pe	Péclet number
Pe_h	thermal Péclet number
Q	constant in the Langmuir isotherm model ($mg\,g^{-1}$) related to the adsorptive capacity
$Q(\pi/\omega)$	reservoir displacement volume (cm^3)
Q_c	flow-rate of the fluid in the column during the cold half-cycle ($mL\,min^{-1}$)
Q_h	flow-rate of the fluid in the column during the cold half-cycle ($mL\,min^{-1}$)
Q_{BP}	flow-rate of removing the product from the bottom reservoir ($mL\,min^{-1}$)
Q_{TP}	flow-rate of removing the product from the top reservoir ($mL\,min^{-1}$)
q	phenol adsorbed per dry mass of adsorbent at a certain time ($mg\,g^{-1}$)
q^*	phenol adsorbed per dry mass of adsorbent in equilibrium with the phenol concentration in solution at a certain time ($mg\,g^{-1}$)
q_e	phenol adsorbed per dry mass of adsorbent at equilibrium ($mg\,g^{-1}$)
Re	Reynolds number
r_p	radius of the particle of the adsorbent (m)
t	time (min)
t_c	cold half-cycle time (min)
t_h	hot half-time (min)
T	absolute temperature (K)
T_c	feeding temperature during the cold half-cycle (K)
T_h	feeding temperature during the hot half-cycle
T_{amb}	ambient temperature (K)
U	feed flow-rate ($cm^3\,min^{-1}$)
u_0	superficial velocity ($m\,min^{-1}$)
u_i	interstitial velocity ($m\,min^{-1}$)
V	volume of the solution (L)
V_U	volume withdrawn as top product per cycle (L)
V_A	molar volume of solute a at its normal boiling temperature ($cm^3\,g\,mol^{-1}$)
W	dry weight (g) of the corresponding adsorbent
z	axial coordinate in the bed (cm)
Z^*	normalized axial coordinate in the bed

Greek letters

ε	bed porosity
ε_p	porosity of the adsorbent
ϕ	dimensionless association factor of solvent B
ϕ_B	fraction of the $Q(\pi/\omega)$ that is withdrawn as bottom product
ϕ_T	fraction of the $Q(\pi/\omega)$ that is withdrawn as top product
η	viscosity of the solution (Pa s)
η_B	viscosity of solvent B (cp)
Ω	LDF factor, which is equal to 3, 8 or 15 for slab, cylindrical or spherical geometry
ρ	density of the adsorbent ($g\,L^{-1}$)
ρ_f	density of the fluid ($g\,L^{-1}$)
τ	tortuosity of the adsorbent
ω	frequency of temperature change

at the top reservoir and a solute-free stream in the bottom one.

The bases of parametric pumping were established in the late 1960s [8–10], when it was seen as a way to purify valuable compounds. It was not until 1980s that parametric pumping was considered for wastewater purification purposes [11] giving the starting point to other works carried out in our laboratory [12–15].

Whether the problem is isolating or purifying a substance of commercial interest or cleaning wastewater, the technology to separate and purify molecules of choice is of critical importance.

The interest of parametric pumping for the wastewater treatment is that this technology would enable purification of industrial wastewaters avoiding the use of chemical regenerant agents and allowing the recycling of the concentrated stream for the industrial process so contributing to achieve the concept of zero-pollutant plant.

In this work, two polymeric resins (Sephabeads SP206 and SP207) and an activated charcoal (Filtrasorb F400) were tested in order to find out their adsorptive performance when removing phenol from wastewater. Thermal parametric pumping being based on the variation of temperature, both batch equilibrium and fixed bed testes were carried out at three different temperatures (293, 310 and 333 K) for each of the adsorbents in order to study the effect of temperature on the adsorption of phenol.

The final aim of the work is to use parametric pumping for the purification of phenolic wastewater and to compare experimental with simulated results obtained by a simulation package of parametric pumping cycles previously developed [15].

2. Experimental

2.1. Chemicals and adsorbents

Phenol (C_6H_6O) was purchased from Sigma–Aldrich (Spain). The adsorption of phenol from aqueous solutions onto activated carbon and polymeric resins was compared. The solutions of phenol were prepared with degassed and distilled water.

The activated carbon used was Filtrasorb F400, which was kindly provided by Chemviron Carbon (Belgium), and the non-ionic polymeric resins were Sephabeads SP206 and SP207 (Mitsubishi Chemical Corporation), which were purchased from Resindion (Italy). These resins have been previously used successfully for phenolic derivatives adsorption [14].

In Table 1, appear the physical characteristics ascertained by the producers for the adsorbents employed in this research work. As it may be seen, the polymeric adsorbents properties are very different from those of the activated charcoal.

2.2. Batch adsorption studies

Adsorption equilibrium experiments were carried out by contacting a given amount of adsorbent with 100 mL of phenol solution in 250 mL Erlenmeyer flasks. Initial concentration of the solution was around 500 mg L^{-1}. Adsorption equilibrium isotherms were measured by batch equilibration placing the volumetric flasks in a shaking mixer at 150 rpm and using a thermostatic bath for temperature control.

Equilibrium experiments were run at 293, 310 and 333 K for each adsorbent–phenol system. After shaking during 48 h, the solution was separated from the adsorbent and the final concentration of phenol in solution was determined by measuring the absorbance at a wavelength of 272 nm by means of a UV–vis spectrophotometer Jasco (model 7800, Japan). The amount of phenol adsorbed onto the different adsorbents, q_e (mg g^{-1}), was calculated by a mass balance relationship (Eq. (1)).

$$q_e = (C_0 - C_e)\frac{V}{W} \quad (1)$$

where C_0 (mg L^{-1}) and C_e (mg L^{-1}) are the initial and equilibrium liquid phase concentrations of phenol, V the volume of the solution (L) and W is the dry weight (g) of the adsorbent.

2.3. Fixed bed adsorption experiments

The adsorbents previously used in batch testes were also used in fixed bed operation. A peristaltic pump Watson–Marlow was used to pump the phenol solution through the beds of the adsorbents here considered. The temperature of the feeding solution was maintained by a thermostatic bath (Edmund Bühler). Phenol concentration at the column outlet was spectrophotometrically determined at 272 nm by an UV–vis spectrophotometer Jasco (model 7800, Japan).

Fixed bed adsorption of phenol onto each adsorbent was studied at three different temperatures: 293, 310 and 333 K. Runs at two different flow-rates were carried out for each of the adsorbents and each of the temperatures. The flow-rates of the feed solution were 10 and 15 mL min^{-1} for Filtrasorb F400 and 10 and 5 mL min^{-1} for both the Sephabeads. The feed concentration was always around 100 mg L^{-1} of phenol. The height of the bed used in the experiments was 300 mm for the polymeric adsorbents and 100 mm for the activated

Table 1
Physical properties of adsorbents used for phenol adsorption

Adsorbent	Filtrasorb F400	Sephabeads SP206	Sephabeads SP207
Matrix	Agglomerated coal based granular activated carbon	Aromatic porous resin with hydrophobic substituents	Aromatic porous resin with hydrophobic substituents
Physical form	Black granular carbon	Yellow opaque beads	Brown opaque beads
Humidity factor (f_h)	1	0.5	0.5
Specific surface area ($m^2\ g^{-1}$)	1050	556	627
Density (g L^{-1})	700	1190	1180
Particle size (mm)	0.7	0.4	0.4

carbon. The diameter of the beds was 10 mm in all cases. The experimental data so obtained were compared with the simulated results from the modelling of the experimental conditions.

2.4. Parametric pumping operation

Fig. 1 shows the pilot plant used to carry out the phenol purification by thermal parametric pumping. This is a completely automated system and it has been described with detail elsewhere [13]. Basically, the core is a borosilicate column (90 mm × 1000 mm) where the adsorbent is packed. Temperature waves in the cycles are measured by thermocouples installed in the column. The solution is pumped through the column downward (cold half-cycle: 293 K) and upward (hot half-cycle: 333 K) alternatively by using the peristaltic pumps 15 or 16, respectively. The solenoid valves 11 and 12 are one open and the other closed while downward flow and on the contrary during the upward flow. Heating and cooling of the fluid phase are carried out by the hot 7 and the cold 6 heat exchangers. There are three reservoirs: top, bottom and feed reservoirs. The top and bottom reservoirs receive product when the solution is pumped through the column in upward or downward flow, respectively. From the feed reservoir, the feed solution is passed into the top reservoir, with the pump 18 on. Pressure transducers installed at the bottom of the reservoirs allow detecting when all the solution contained in a reservoir was transferred, which means one half-cycle ending. Bottom and top products were collected at fixed time intervals by a fraction collector, with pumps 19 and 17 working. The solute concentration is later determined spectrophotometrically.

In this work, the experimental set-up above described was used for the system water–phenol–Sephabeads SP206, other systems having been previously managed [12–14]. Previously to the cyclic operation of the system, fixed bed adsorption runs were carried out in the pilot unit at both 293 and 333 K using Sephabeads SP206 as adsorbent. The feed concentration was around 500 mg L^{-1} and the flow-rate 600 mL min^{-1}, the height and the diameter of the SP206 bed being 800 and 90 mm, respectively. Previously to each run, the temperature of the bed was stabilized by pumping

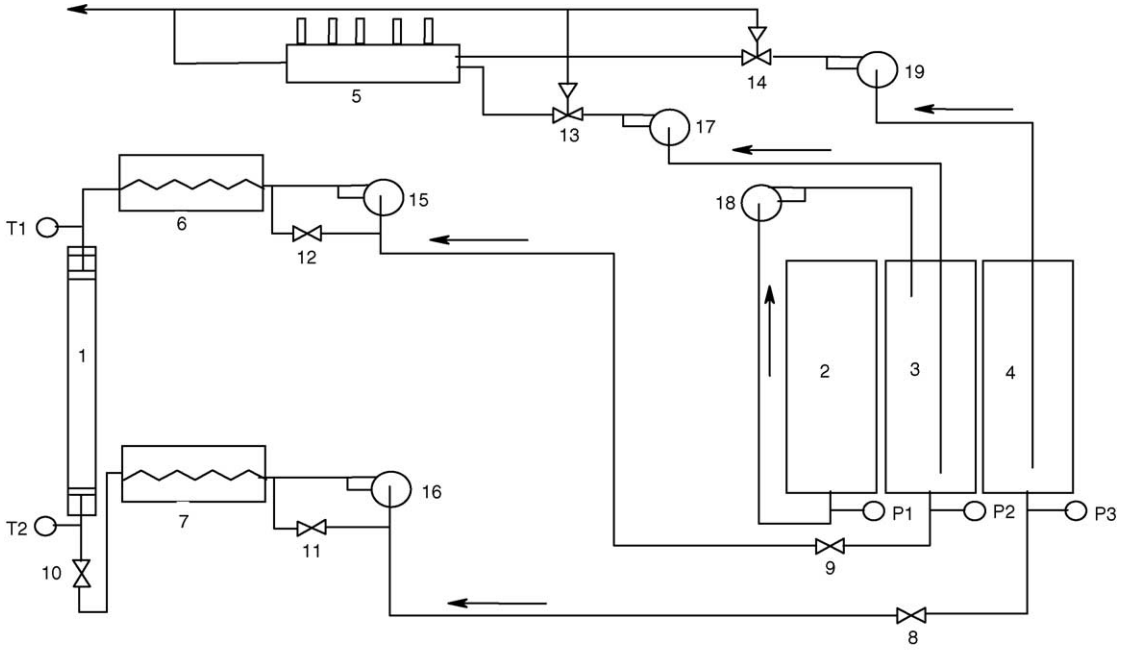

Legend: (1) glass column G90-Amicon; (2) feed reservoir;
(3) top reservoir;(4) bottom reservoir;
(5) fraction collector Gilson; (6) and (7) heat exchangers;
(8)-(12) two-ways solenoid valves;
(13) and (14) three-ways solenoid valves;
(15) and (16) peristaltic pumps Watson Marlow;
(17)-(19) peristaltic pumps Gilson; (T1) and (T2) thermocouples (type K);
(P1)-(P3) pressure transducers Schaevitz (type P510).

Fig. 1. Experimental set-up of the parametric pumping pilot plant. Legend: (1) glass column G90-Amicon; (2) feed reservoir; (3) top reservoir; (4) bottom reservoir; (5) fraction collector Gilson; (6 and 7) heat exchangers; (8–12) two-ways solenoid valves; (13 and 14) three-ways solenoid valves; (15 and 16) peristaltic pumps Watson Marlow; (17–19) peristaltic pumps Gilson; (T1 and T2) thermocouples (type K); (P1–P3) pressure transducers Schaevitz (type P510).

deionised water at 600 mL min^{-1} and at 293 or 333 K to later carry out the corresponding phenol isothermal fixed bed saturation.

The operation of the parametric pumping pilot plant was performed during 10 cycles in a recuperative mode. The regime of operation was semi-continuous, i.e., the sequence was: feed input and top product withdrawal during the upward hot half-cycle and bottom product withdrawal during the downward cold half-cycle. A simulation package [15] was used for the simulation of the cyclic operation. Experimental results were compared with the simulated ones obtained using a non-isothermal model, which includes Linear Driving Force (LDF) describing intraparticle mass transfer and axial dispersion.

3. Results and discussion

3.1. Adsorption isotherms

The adsorption equilibrium isotherms for phenol onto each adsorbent at various temperatures, q_e (mg g^{-1}), versus the adsorbate liquid concentration at equilibrium, C_e (mg L^{-1}), were fitted with the Langmuir equation.

Langmuir equation (2) is based on a theoretical model where the maximum adsorption capacity corresponds to a monolayer saturated with adsorbate molecules on the adsorbent surface, which is energetically homogeneous.

$$q_e = \frac{Q K_L C_e}{1 + K_L C_e} \quad (2)$$

where Q is a constant relative to the adsorptive capacity and K_L is the parameter which relates to the adsorption energy [16].

$$K_L = K_L^{\infty} \exp\left(-\frac{\Delta H_L}{RT}\right) \quad (3)$$

Fittings have been calculated by MATLAB 6.1 following the optimization routine and using the Simplex direct search method. The characteristic parameters corresponding to the fittings are shown in Table 2. The Q corresponding to the Filtrasorb is higher than this corresponding to the Sephabeads SP206 and SP207. On the contrary, the process is more exothermic in the case of phenol adsorption onto the polymeric resins than onto the activated charcoal as indicated by the value of ΔH_L.

Table 2
Equilibrium parameters determined for the adsorption of phenol onto Filtrasorb F400, Sephabeads SP206 and SP207

Langmuir parameters	Filtrasorb F400	Sephabeads SP206	Sephabeads SP207
Q (mg g^{-1})	169.1	85.0	88.8
K_L^{∞} (L mg^{-1})	1.32×10^{-3}	1.52×10^{-8}	2.99×10^{-7}
ΔH_L (kJ mol^{-1})	−12.12	−30.35	−23.22

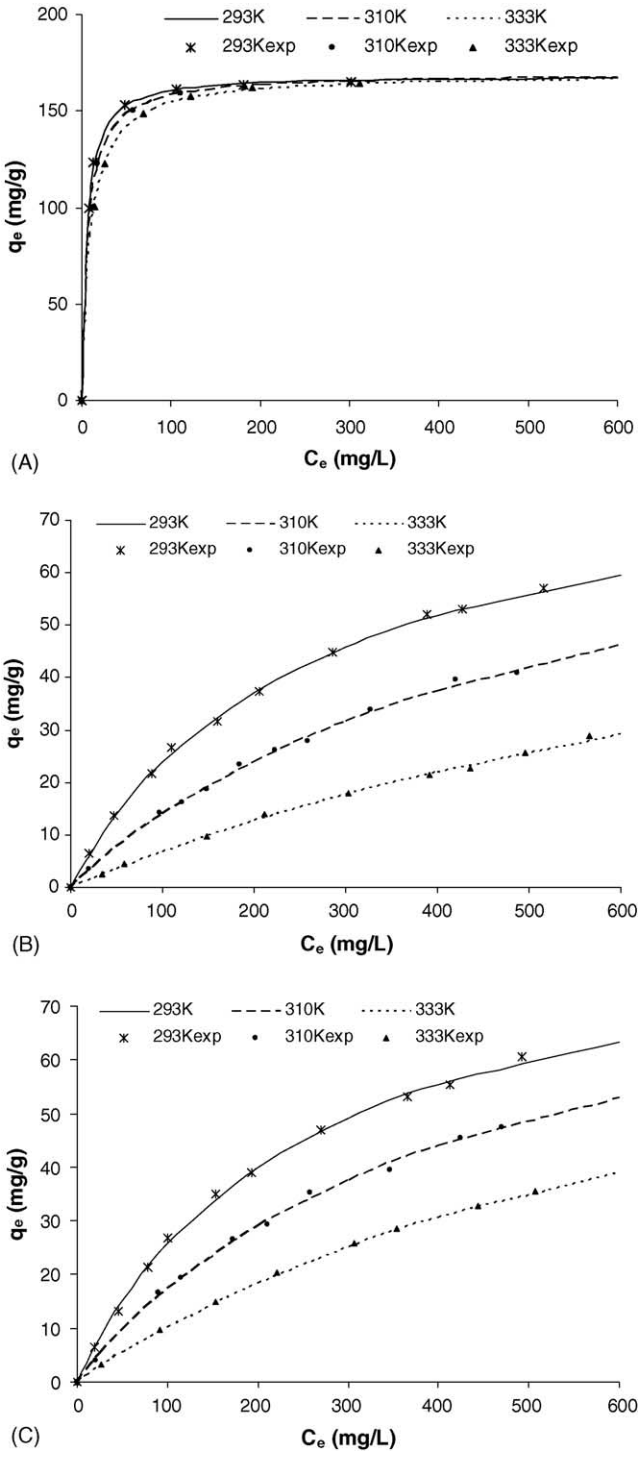

Fig. 2. Experimental adsorption equilibrium (symbols), q_e vs. C_e, and fittings to Langmuir model (lines) at different temperatures (293, 310 and 333 K) for the adsorption of phenol onto Filtrasorb F400 (A), Sephabeads SP206 (B) and Sephabeads SP207 (C).

The experimental adsorbed concentrations as a function of liquid phase concentration corresponding to the phenol adsorption by each of the adsorbents at each of the temperatures considered are shown in Fig. 2. The obtained fittings to the

Langmuir model are shown together with the experimental points.

The adsorptive capacity of phenol is much higher for the activated carbon Filtrasorb F400 than for the polymeric resins. Nevertheless, the influence of temperature on equilibrium is much more noticeable in the case of the adsorption of phenol onto the resins, especially onto Sephabeads SP206.

From the equilibrium results, it may be found the separation to be expected as a function of temperature for each of the systems phenol–adsorbent. Table 3 shows for each of the adsorbents considered the corresponding *separation parameter* (b) regarding to the adsorption of phenol. The parameter b, introduced by Pigford et al. [10], is indicative of the separation potential:

$$b = \frac{a}{1 + \bar{m}} \tag{4}$$

where the average slope $\bar{m} = \frac{m(T_1)+m(T_2)}{2}$ and the deviation $a = \frac{m(T_1)-m(T_2)}{2}$, considering $T_1 < T_2$.The capacity parameter here appearing is defined as

$$m(T) = \frac{(1-\varepsilon)\rho f_h K(T)}{\varepsilon},$$

where $K(T) = QK_L$ and K_L was the Langmuir equilibrium constant $K_L(T)$ corresponding to each temperature (see Table 2), ρ and f_h the density and the humidity factor of the corresponding adsorbent, which appear in Table 1, and ε is the bed porosity, which was 0.4 in this work.

As it may be observed in Table 3, in the temperature range studied, the largest b values correspond to the adsorption of phenol onto Sephabeads SP206.

3.2. Fixed bed adsorption

The breakthrough curves corresponding to the different experimental conditions were obtained for each of the adsorbents. The mathematical model considers the mass balance in the liquid phase, the non-linear Langmuir isotherm and the mass transfer governed by the Linear Driving Force rate.

3.2.1. Mass balance (equation of the bed)

The mass balance in a bed volume element is:

$$D_{ax}\frac{\partial^2 C(z,t)}{\partial z^2} - u_i\frac{\partial C(z,t)}{\partial z} = \frac{\partial C(z,t)}{\partial t} + \frac{1-\varepsilon}{\varepsilon}\rho f_h \frac{\partial \langle q(z,t)\rangle}{\partial t} \tag{5}$$

Table 3
Separation parameter, b corresponding to the different systems adsorbent–phenol

	Temperature range (K)		
	293–310	310–333	293–333
Filtrasorb F400	0.14	0.16	0.29
Sephabeads SP206	0.33	0.39	0.63
Sephabeads SP207	0.26	0.30	0.52

where D_{ax} is the axial dispersion, u_i the interstitial velocity, ε the bed porosity, z the axial position, C the concentration in the bulk fluid phase and $\langle q\rangle$ is the average adsorbed phase concentration in the adsorbent particles.

3.2.2. Adsorption equilibrium isotherm

The adsorption equilibrium is described by the Langmuir isotherm:

$$q^*(z,t) = \frac{QK_L C(z,t)}{1 + K_L C(z,t)} \tag{6}$$

$$K_L = K_L^{\infty} \exp\left(-\frac{\Delta H_L}{RT}\right) \tag{7}$$

3.2.3. Mass transfer

The Linear Driving Force approximation is used to describe intraparticle mass transfer:

$$\frac{\partial \langle q(z,t)\rangle}{\partial t} = k_{LDF}[q^*(z,t) - \langle q(z,t)\rangle] \tag{8}$$

where k_{LDF} is the Linear Driving Force kinetic constant and $q^*(z, t)$ is the adsorbed phase concentration in equilibrium with the bulk concentration $C(z, t)$.

The boundary conditions for the mass balance equation (5) are the Danckwerts boundary conditions:

$$z = 0, \qquad D_{ax}\frac{\partial C(z,t)}{\partial z}|_{z=0} = u_i(C(0,t) - C_0) \tag{9}$$

$$z = L, \qquad \frac{\partial C(z,t)}{\partial z}|_{z=L} = 0 \tag{10}$$

The associated initial conditions for the adsorption bed are:

$$C(z,0) = 0 \tag{11}$$

$$q(z,0) = 0 \tag{12}$$

The axial dispersion was obtained from the following expression [17]:

$$\frac{u_0 d_p}{D_{ax}} = (0.2 + 0.011 Re^{0.48}) \tag{13}$$

with

$$Re = \frac{u_i \rho_s \varepsilon d_p}{\eta} \tag{14}$$

The values of the Reynolds and Péclet number and the calculated axial dispersion D_{ax} are shown in Table 4.

The k_{LDF} used in the models are shown in Table 5 and were estimated by the following expression [18], based on the equivalence of LDF models for homogeneous and porous particles:

$$k_{LDF} = \frac{\Omega D_{pe}}{\rho f_h r_p^2 \frac{dq^*}{dC}} \tag{15}$$

where D_{pe} ($m^2\ min^{-1}$) is the effective pore diffusivity, r_p (m) the radius of the particle of the adsorbent, Ω the LDF factor,

Table 4
Parameters used for estimating the D_{ax} corresponding to the different fixed bed systems considered

Adsorbent	T (K)	L (mm)	Flow-rate (mL min^{-1})	Re	D_{ax} (cm^2 min^{-1})
Filtrasorb F400	293	100	10	1.45	4.18
	310			2.31	4.12
	333			3.13	4.07
Sephabeads SP206	293	300	10	0.46	1.35
	310			0.73	1.34
	333			0.98	1.33
Sephabeads SP207	293	300	10	0.46	1.35
	310			0.73	1.34
	333			0.98	1.33

which is equal to 15 for spherical particles [18], ρ the density of the adsorbent, f_h humidity factor and $(\frac{dq^*}{dC})$ is the slope of the equilibrium data.

The LDF approximation is valid for cyclic processes with long cycle times as is the case of parametric pumping; in fact the half-cycle time is higher than $1.5/k_{LDF}$ [19].

The D_{pe} (m^2 min^{-1}) was calculated as [20]:

$$D_{pe} = \frac{\varepsilon_p D_m}{\tau} \quad (16)$$

where D_m (m^2 min^{-1}) is the molecular diffusivity of phenol in water, τ the tortuosity of the adsorbent and ε_p is its porosity.

The molecular diffusivity of phenol in water D_m was estimated, after the corresponding unit transformations, according to the Wilke–Chang [21] method:

$$D_m = 7.4 \times 10^{-8} \frac{(\phi M_B)^{1/2} T}{\eta_B V_A^{0.6}} \quad (17)$$

where V_A is the molar volume of the solute, the value of $V_A = 108\,cm^3\,g\,mol^{-1}$ for phenol was estimated by the Le Bas additive method [22]. Wilke and Chang recommended that ϕ be chosen 2.6 if the solvent is water and the viscosity of water η_B at the corresponding temperature was used.

Table 5
LDF kinetic rate constants estimated (k_{LDF}) for the adsorption of phenol onto each adsorbent

Adsorbent	T (K)	D_m (m^2 min^{-1})	ε_p	τ	D_{pe} (m^2 min^{-1})	k_{LDF} (min^{-1})
Filtrasorb F400	293	5.34E−08	0.75	2	2.00E−08	0.027
	310	8.88E−08			3.33E−08	0.036
	333	1.32E−07			4.95E−08	0.054
Sephabeads SP206	293	5.34E−08	0.61	2	1.63E−08	0.074
	310	8.88E−08			2.71E−08	0.192
	333	1.32E−07			4.03E−08	0.409
Sephabeads SP207	293	5.34E−08	0.63	2	1.68E−08	0.053
	310	8.88E−08			2.80E−08	0.148
	333	1.32E−07			4.16E−08	0.330

The partial differential equations of the model were solved using the software package *gPROMS*® for *g*eneral *PRO*cess *M*odelling *S*ystem. The orthogonal collocation method on finite elements (OCFE) was used with 50 finite elements and

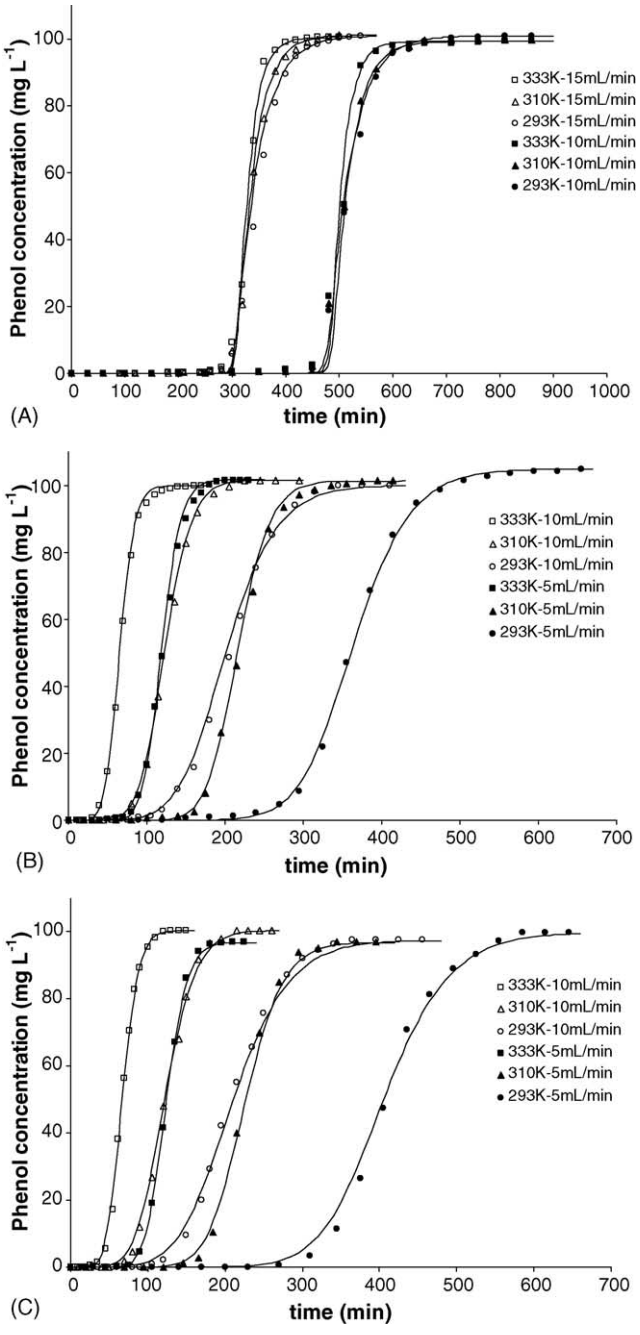

Fig. 3. Fixed bed adsorption of phenol onto Filtrasorb F400 (A), Sephabeads SP206 (B) and Sephabeads SP207 (C). The bed length was 100 mm for Filtrasorb F400 and 300 mm for Sephabeads SP206 and SP207 and solution was fed at three temperatures (293, 310 and 333 K) at each of two different flow-rates. Symbols correspond to the experimental results and full lines to the simulated ones.

2 interior collocation points in each element of the adsorption bed.

Experimental data are shown together with the simulated ones in Fig. 3. The LDF model seems to well describe the fixed bed adsorption of phenol onto the adsorbents here used at the conditions of temperature and flow-rate here studied.

As it may be seen in Fig. 3, the lower the flow-rate the longer breakthrough times; anyway, for the three adsorbents used in this work at both the flow-rates tested, a constant-pattern along the column was achieved.

The breakthrough curves corresponding to the different adsorbents here considered confirm that the influence of temperature variable on the adsorption of phenol is much more noticeable for the polymeric resins Sephabeads than for the activated carbon Filtrasorb F400. This can be seen by comparing runs at the same flow-rate (10 mL min^{-1}) in Fig. 3A (Filtrasorb 400) and Fig. 3B and C (Sephabeads SP206 and SP207, respectively).

3.3. Parametric pumping operation and simulation

From the batch and fixed bed tests results, the adsorbent Sephabeads SP206 is the one which adsorption performance is affected by temperature in a higher degree. Recuperative thermal parametric pumping being based in differences on adsorption capacity caused by changes in the temperature of the solution, this resin was selected for studying phenol purification by parametric pumping.

Fixed bed adsorption of phenol at 293 and at 333 K was carried out in the column of the parametric pumping set-up using a bed of Sephabeads SP206 (800 mm × 90 mm). Fig. 4 shows the experimental results together with those simulated by the model previously used in lab-scale columns. This model well predicts the fixed bed adsorption of phenol onto Sephabeads SP206 also at a pilot scale.

About the parametric pumping system Sephabeads SP206–phenol, experimental results were compared with the simulated ones using a Linear Driving Force model with axial dispersion. Equations corresponding to the model used include, apart of the mass balance (Eq. (5)), the equilibrium isotherm (Eqs. (6) and (7)) and the mass transfer (Eq. (8)), an energy balance and the balance equations of the reservoirs:

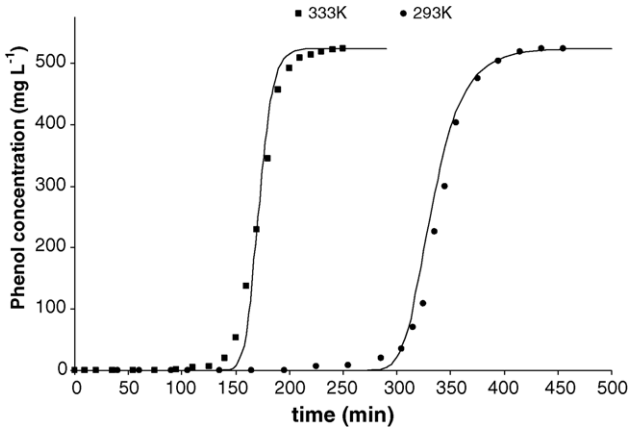

Fig. 4. Fixed bed adsorption of phenol onto Sephabeads SP206 in pilot scale (800 mm × 90 mm). The solution was feed at a flow-rate of 600 mL min^{-1} and two runs, at 293 and 333 K, respectively, were carried out.

3.3.1. Energy balance

$$[\rho_f Cp_f \varepsilon + \rho Cp_s(1-\varepsilon)]\frac{\partial T(z,t)}{\partial t} = K_{ae}\frac{\partial^2 T(z,t)}{\partial z^2} \pm \rho_f Cp_f u_0 \frac{\partial T(z,t)}{\partial z} - h_w A_w (T - T_{amb}) + (-\Delta H)\frac{\partial \langle q(z,t)\rangle}{\partial t} \quad (18)$$

where K_{ae} is the axial thermal conductivity, h_w the heat transfer coefficient of the wall of the column, A_w the wall specific area, ρ_f and ρ the densities of the fluid and of the adsorbent, and Cp_f and Cp_s are the heat capacities of the fluid

Table 6
Characteristic parameters of the operated parametric pumping system

Properties of the resin
- $\rho = 1190\ g\ L^{-1}$
- $f_h = 0.5$
- $r_p = 2 \times 10^{-4}$ m
- $\varepsilon_p = 0.607$
- $\tau = 2$

Operating variables
- $T_c = 293$ K
- $T_h = 333$ K
- $T_{amb} = 298$ K
- $V_U = 17000$ mL
- $Q(\pi/\omega) = 20000$ mL
- $\phi_B = 0.15$
- $\phi_T = 0.25$
- $t_c = 85$ min
- $t_h = 100$ min
- $Q_c = 200\ mL\ min^{-1}$
- $Q_h = 200\ mL\ min^{-1}$
- $Q_{TP} = 62.5\ mL\ min^{-1}$
- $Q_{BP} = 32\ mL\ min^{-1}$
- $C_F = 544\ mg\ L^{-1}$

Model parameters
- $Pe = 120$
- $Pe_h = 100$

Bed characteristics
- $L = 800$ mm
- $D = 90$ mm
- $\varepsilon = 0.4$

Transport parameters
- $D_m(293\ K) = 1.32 \times 10^{-7}\ m^2\ min^{-1}$
- $D_m(333\ K) = 5.34 \times 10^{-8}\ m^2\ min^{-1}$
- $h_w = 0.852\ kJ/(m^2\ s\ K)$

Equilibrium parameters
- $Q = 85\ mg\ g^{-1}$
- $K_L^{\infty} = 1.524 \times 10^{-8}\ L\ mg^{-1}$
- $\Delta H_L = 30353\ J\ mol^{-1}$

and of the adsorbent, respectively. Considering $z = 0$ at the bottom of the column and $z = L$ at the top, in Eq. (5), the term $\pm\rho_f Cp_f u_0 \frac{\partial T(z,t)}{\partial z}$ has the "+" sign for the cold half-cycle downwards, and the "−" sign for the hot half-cycle upwards.

3.3.2. Balance of the reservoirs

- Hot half-cycle:

$$\langle C_{BP}\rangle = \langle C_{BP}\rangle_{n-1} \tag{19}$$

$$\langle C_{TP}\rangle = \frac{(1-\phi_B)\langle C(L,t)\rangle_n}{(1+\phi_T)} + C_F\frac{\phi_B+\phi_T}{1+\phi_T} \tag{20}$$

where $\langle C_{BP}\rangle$ and $\langle C_{TP}\rangle$ are the average concentration of phenol in the fluid which is in the bottom and in the top reservoirs, respectively, ϕ_B and ϕ_T the fractions of the total reservoir displacement volume ($Q(\pi/\omega)$) that are withdrawn as product from the bottom and the top reservoirs, respectively, and n refers to the number of cycles.

- Cold half-cycle:

$$\langle C_{BP}\rangle = \langle C(0,t)\rangle_n \tag{21}$$

The boundary conditions for the equations included in the parametric pumping model are:

- Hot half-cycle:

$$z = 0, \qquad C(0,t) = \langle C_{BP}\rangle_n \tag{22}$$

$$T = T_h \tag{23}$$

$$z = L, \qquad \frac{\partial C(z,t)}{\partial z} = 0 \tag{24}$$

$$\frac{\partial T(z,t)}{\partial z} = 0 \tag{25}$$

- Cold half-cycle:

$$z = 0, \qquad \frac{\partial C(z,t)}{\partial z} = 0 \tag{26}$$

$$\frac{\partial T(z,t)}{\partial z} = 0 \tag{27}$$

$$z = L, \qquad C(L,t) = \langle C_{TP}\rangle_n \tag{28}$$

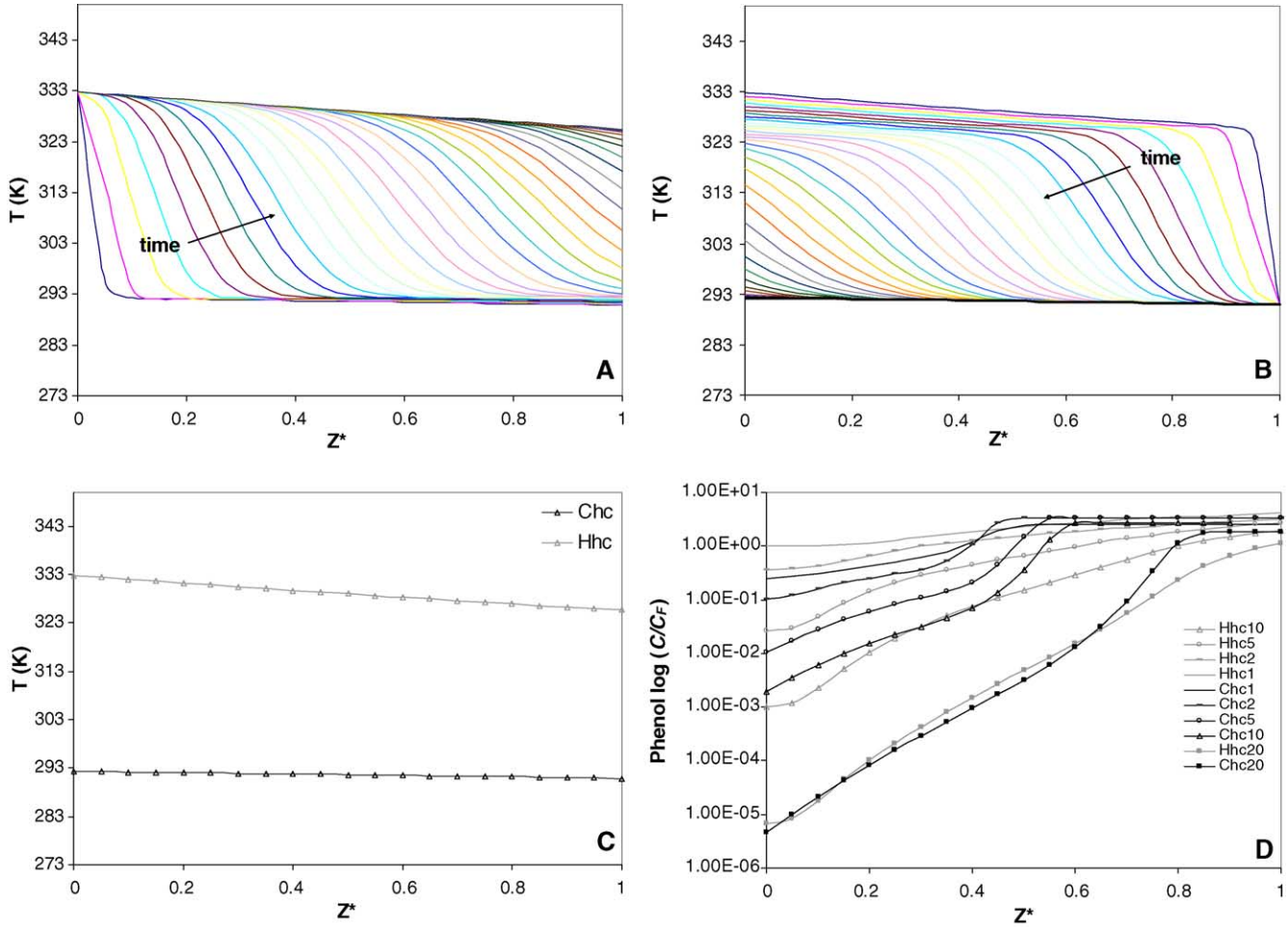

Fig. 5. Profiles of temperature and concentration during the operation of parametric pumping for phenol wastewater purification. (A) Bed temperature profile evolution along the 10th hot half-cycle. (B) Bed temperature profile evolution along the 10th cold half-cycle. (C) Bed temperature profiles at the end of the hot half-cycle (Hhc) and at the end of the cold half-cycle (Chc). (D) Concentration profiles in the bed at the end of the hot and cold half-cycles for cycles 1, 5 and 10.

$$T = T_c \tag{29}$$

The initial conditions were:

$$t = 0, \qquad C(z, 0) = C_F \tag{30}$$

$$T(z, 0) = T_c \tag{31}$$

The characteristic parameters of the operated system and the conditions under which the parametric pumping runs were carried out are shown in Table 6. Fig. 5 shows the simulated axial profiles of temperature and concentration corresponding to the operation of the parametric pumping unit under these conditions. The evolution of the temperature profile along the time of the 10th hot half-cycle and the 10th cold half-cycle may be seen in Fig. 5A and B, respectively. The temperatures along the bed at the end of the hot and at the end of the cold half-cycles are in Fig. 5C. In Fig. 5D, the simulated concentration profiles of phenol at the end of the hot and cold half-cycles are shown for cycles 1, 5 and 10. These historic profiles reflect the evolution of the concentration waves during the operation of the parametric pumping system.

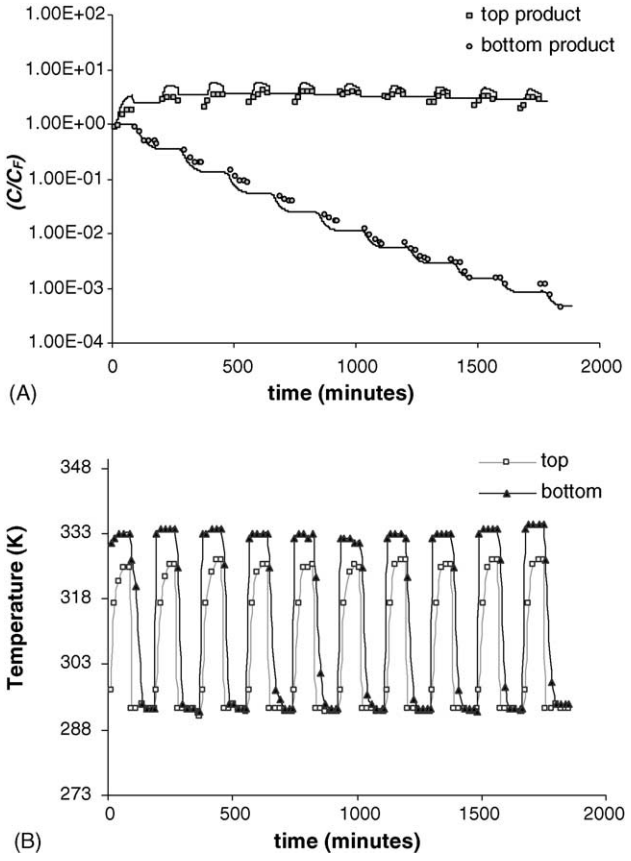

Fig. 6. (A) Experimental results (symbols) of the parametric pumping run for the system phenol/water/SP206 together with the model predictions (full lines). Top and bottom product normalized phenol concentrations, C/C_F, are shown as a function of time in recuperative parametric pumping. (B) History of top and bottom temperatures during the recuperative parametric pumping.

Finally, the experimental results corresponding to the operation of the parametric pumping set-up are shown in Fig. 6A together with the predictions of the LDF model. The top and bottom concentrations of phenol are represented as a function of time. As it may be seen, the simulation predictions are in good agreement with experimental results, which confirms that the Linear Driving Force approximation is appropriate for describing mass transfer in this cyclic process. The experimental top and bottom temperatures in the bed are shown in Fig. 6B along the 10 cycles of operation.

At the end of the hot and the cold 10th half-cycles the concentrations in the top and the bottom reservoirs were, respectively, 1560 and 0.2 mg L^{-1}. A high level of purification was obtained and, the concentration of phenol in the bottom reservoir was $C/C_F < 0.001$ from the 10th cycle. The top effluent reached concentrations of phenol three times that of the feed and so the concentration in the top reservoir.

4. Conclusions

Adsorption of phenol onto polymeric resins (Sephabeads SP206 and SP207) and activated carbon (Filtrasorb F400) was studied. Batch testes were carried out in order to make a screening of adsorbents related to the effect of temperature on the adsorptive behaviour. On the basis of the separation parameter *b*, Sephabeads SP206 showed the higher separation potential in function of temperature for the adsorption of phenol. Dynamic studies were also done for the adsorption of phenol onto the polymeric resins and onto the activated carbon to ascertain the applicability of the LDF model in fixed bed. The effect of temperature on the fixed bed adsorption of phenol was also more noticeable for the polymeric resins, especially for Sephabeads SP206, rather than for the Filtrasorb F400.

Pilot scale fixed bed using Sephabeads SP206 as adsorbent was studied before operating the parametric pumping unit. Model equations including intraparticle mass transfer described by the LDF model satisfactorily predicted the breakthrough curves at pilot scale (in an 800 mm × 90 mm bed) carried out both at 293 and 333 K.

Thermal parametric pumping in recuperative mode was performed in a pilot plant using Sephabeads SP206 for phenol adsorption. By applying a $T_c = 293$ K and a $T_h = 333$ K a high level of purification was obtained; the concentration of phenol in the bottom reservoir was going down and $C/C_F < 0.001$ from the 10th cycle, the $C_F = 544$ mg L^{-1}. It was seen that the purification of liquid streams containing phenol may be achieved by thermal parametric pumping using Sephabeads SP206 as adsorbent. Top and bottom concentrations of phenol as a function of time were predicted using a model including a mass balance, an energy balance, the equilibrium isotherm and the Linear Driving Force approximation for describing intraparticle mass transfer, which satisfactorily simulated the experimental results.

Acknowledgements

This research has been supported by a Marie Curie Fellowship of the European Community Fifth Framework Programme's Human Resources and Mobility (HRM) under Contract number EVK1-CT-2002-50018. Financial support of M. Zabkova from FCT (SFRH/BD/8007/2002) is also gratefully acknowledged.

References

[1] S.A. Bryant, T.W. Schultz, Toxicological assessment of biotransformation products of pentachlorophenol: tetrahymena population growth impairment, Arch. Environ. Contam. Toxicol. 26 (1994) 299.
[2] K.J. Abburi, Adsorption of phenol and *p*-chlorophenol from their single and bisolute aqueous solutions on Amberlite XAD-16 resin, J. Hazard Mater. B 105 (2003) 143.
[3] K. Knaebel, The basics of adsorber design, Chem. Eng. 106 (1999) 92.
[4] A. Kumar, S. Kumar, S. Kumar, Adsorption of resorcinol and catechol on granular activated carbon: equilibrium and kinetics, Carbon 41 (2003) 3015.
[5] N. Roostaei, F. Handan Tezel, Removal of phenol from aqueous solutions by adsorption, J. Environ. Manage. 70 (2004) 157.
[6] G. Simon, G. Grevillot, L. Hanák, T. Szánya, G. Marton, Theoretical study of adsorptive parametric pumping and swing chromatography with flow reversal, Chem. Eng. J. 70 (1998) 71.
[7] N.M. Ghasem, Combined mode operation for thermal parametric pumping, J. Chem. Technol. Biotechnol. 78 (2003) 666.
[8] R.H. Wilhelm, A.W. Rice, A.R. Bendelius, "Parametric pumping", a dynamic principle for separating fluid mixtures, Ind. Eng. Chem. Fundam. 5 (1966) 141.
[9] R.H. Wilhelm, N.H. Sweed, Parametric pumping: separation of mixture of toluene and *n*-heptane, Science 159 (1968) 522.
[10] R.L. Pigford, B. Baker, D.E. Blum, An equilibrium theory of the parametric pumping, Ind. Eng. Chem. Fundam. 8 (1969) 144.
[11] C.A.V. Costa, A.E. Rodrigues, G. Grevillot, D. Tondeur, Purification of phenolic wastewaters by parametric pumping: nonmixed dead volume equilibrium model, AIChE J. 28 (1982) 73.
[12] L.M. Ferreira, A.E. Rodrigues, Adsorptive separation by thermal parametric pumping. Part 1: modeling and simulation, Adsorption 1 (1995) 213.
[13] L.M. Ferreira, A.E. Rodrigues, Adsorptive separation by thermal parametric pumping. Part 2: experimental study of the purification of aqueous phenolic solutions at pilot scale, Adsorption 1 (1995) 233.
[14] S. Díez, A. Leitão, L.M. Ferreira, A.E. Rodrigues, Adsorption of phenylalanine onto polymeric resins: equilibrium, kinetics and operation of a parametric pumping unit, Sep. Purif. Technol. 13 (1998) 25.
[15] R.R. Davesac, L.T. Pinto, F.A. da Silva, L.M. Ferreira, A.E. Rodrigues, A package for thermal parametric pumping adsorptive processes, Chem. Eng. J. 76 (2000) 115.
[16] N.K. Hamadi, X.D. Chen, M.M. Farid, G.Q. Lu, Adsorption kinetics for the removal of chromium(VI) from aqueous solution by adsorbent derived from used tyres and sawdust, Chem. Eng. J. 84 (2001) 95.
[17] G. Guiochon, S.G. Shirazi, A.M. Katti, Fundamentals of Preparative and Nonlinear Chromatography, Academic Press, Boston, 1994.
[18] D.C. Azevedo, Separation/reaction in simulated moving bed, application to the production of industrial sugars, Ph.D. Thesis, Laboratory of Separation and Reaction Engineering, School of Engineering, University of Porto, Portugal, 2001.
[19] R. Yang, Gas Separation by Adsorption Processes, Butterworths, Stoneham, 1987.
[20] R.C. Reid, J.M. Prausnitz, B.E. Poling, The Properties of Gases and Liquid, McGraw-Hill International Editions, New York, 1988.
[21] C.R. Wilke, P. Chang, Correlation of diffusion coefficients in dilute solutions, AIChE J. 1 (1955) 264.
[22] G. Le Bas, The Molecular Volumes of Liquid Chemical Compounds, Longmans, New York, 1915.